ELSEVIER

Materials Science and Engineering B 113 (2004) 24–29

MATERIALS SCIENCE & ENGINEERING B

www.elsevier.com/locate/mseb

Photoluminescence in Si/ZnO nanocomposites

U. Pal[a,*], J. García Serrano[b], N. Koshizaki[c], T. Sasaki[c]

[a] Instituto de Física, Universidad Autónoma de Puebla, Apdo. Postal J-48, Puebla, Pue 72570, México
[b] Centro de Investigaciones en Materiales y Metalurgia, Universidad Autónoma del Estado de Hidalgo, C.U., Carretera Pachuca-Tulancingo Km. 4.5, 42074 Pachuca, Hgo., México
[c] Nanoarchitectonic Research Center, National Institute of Advanced Industrial Sciences and Technology (AIST), Central-5 MITI, 1-1 Higashi, Tsukuba, Ibaraki 305-8565, Japan

Received 5 January 2004; accepted 14 June 2004

Abstract

Composite films of Si and ZnO were prepared by r.f. co-sputtering technique with different Si contents. Photoluminescence (PL) and Raman spectroscopy were used to characterize the films. Transmission electron microscopy revealed that the Si dispersed in the ZnO matrix form nano-particles of size ranging from 2 to 4 nm. On thermal annealing at and above 700 °C, the nano-particles aggregated to form micro-crystals. X-ray photoelectron spectroscopy (XPS) and Raman spectroscopy revealed that the Si in the composite films remain in the SiO_X ($0 < X < 2$) state. With the increase of annealing temperature, the higher oxidation state of Si is revealed. A strong and broad PL peak revealed at around 2.24 eV along with the other emissions. The emission could involve a band-to-band recombination mechanism within Si cores and emission sensitive to surface and/or interface states. Evolution of PL emissions and Raman peaks are discussed on the basis of formation of nano-particles and micro-crystals in the films and variation of oxidation state of Si with annealing temperature.
© 2004 Elsevier B.V. All rights reserved.

Keywords: Nanocomposites; Photoluminescence; Raman; Si–ZnO

1. Introduction

Strong photoluminescence (PL) in the visible spectral region from microstructures made of Si and Ge is presently the subject of intensive research. Since the initial work of Canham [1] on porous Si prepared by anodization of Si wafers, several workers have reported their experimental results on the fabrication methods [2–4], structural characterization [5,6] and optical properties [7–9] of nano- and micro-crystals. The PL properties of Si [7,10] and Ge [11] prepared by various methods have also been reported. Apart from the porous Si work, all the Si and Ge micro-crystals were prepared using SiO_2 as matrix material. In most of the works, the PL in the visible spectral region in the microstructures is claimed to be attributed to quantum size effect in them. However, there is no direct correlation between the PL properties and nanometer-size microstructures and the mechanism of PL is still debatable. Though a blue shift in PL spectra with the decrease of crystallite size in Si nanocrystals is demonstrated by several workers [12,13] a similar shift has not been observed in all the cases [14–16]. Although, theoretical calculations predict the direct nature of optical transitions in nanocrystals [17,18] no experimental evidence of this is available so far.

In the present work, we tried to prepare Si nano-particles in ZnO, a functional matrix material, using r.f. sputtering technique. As the use of functional matrix materials like TiO_2, ZnO, MgO is rather new [19–21], the influence of such photo-active surroundings on the guest-host systems is not yet well understood. As the possible use of Si nanocrystals as a high photon energy luminescence source, we incorporated Si nanocrystals in ZnO matrix, as the new host and examined its luminescence properties for the first time.

The composite films were prepared on quartz glass substrates and annealed at different temperatures (400–800 °C) in vacuum. X-ray photoelectron spectroscopy (XPS) technique is used to study the chemical composition of the films and the chemical state of Si in them. Room temperature PL and Raman scattering techniques were used to study the

* Corresponding author. Tel.: +52 22 2295500; fax: +52 22 2295611.
E-mail address: upal@sirio.ifuap.buap.mx (U. Pal).

0921-5107/$ – see front matter © 2004 Elsevier B.V. All rights reserved.
doi:10.1016/j.mseb.2004.06.008

origin of different luminescence bands and their evolution with the variation of annealing temperature. On the basis of XPS and Raman results, possible mechanisms of the PL emissions were discussed.

2. Experiments

Si/ZnO composite films were deposited on quartz glass substrates (Nihon Rika Garasu Kogyo) by co-sputtering technique using an r.f. sputtering system (Shimadzu HSR-521). Pieces of Si wafers (targets there after) of 5 mm × 5 mm × 0.3 mm size were placed symmetrically on a ZnO target of 100 mm diameter and sputtered with 100 W r.f. power at 10 mTorr Ar gas pressure. In order to vary the concentration of Si in ZnO, the number of Si targets was varied from 4 to 16. The Si and ZnO targets were co-sputtered for a fixed time (60 min) to maintain the thickness of the films more or less same. The thickness of the films varied from 713 to 890 nm. The as-deposited films with different Si content were annealed at 400, 600, 700 and 800 °C temperatures for 5 h in vacuum (2×10^{-6} Torr). The chemical composition of the films and the chemical states of the constituting elements were examined by XPS (PHI 5600ci) technique. PL spectra of the as-deposited and annealed films were recorded by a Shimadzu RF 5300-PC spectrofluorophotometer using the 350 nm emission of a xenon lamp as excitation source. ASPEX Ramalog-10 system with 514.5 nm line of an Ar ion laser as excitation source was used to record the Raman spectra.

3. Results and discussion

Fig. 1 shows the variation of Si content in the as-deposited films prepared with different numbers of Si pieces on the ZnO target. Si content in the films increased with the increase of Si

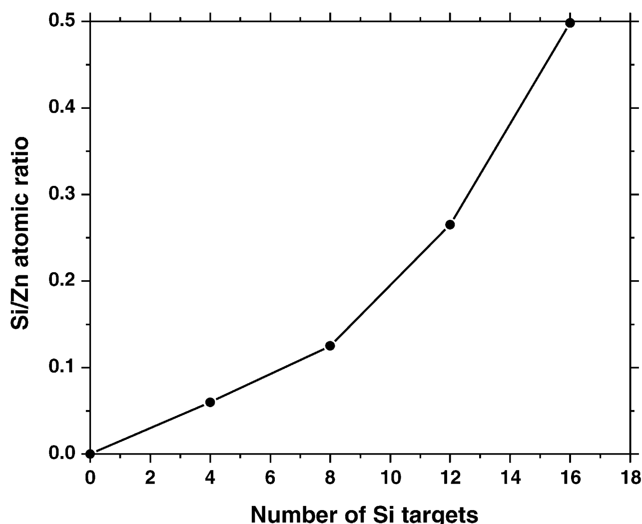

Fig. 1. Variation of Si/Zn atomic ratio with the variation of Si targets.

Fig. 2. TEM photograph of as-deposited Si/ZnO film prepared with 12 Si targets.

pieces. The Si in the composite films remained in the SiO_X ($0 < X < 2$) chemical state with its Si_{2P} peak position in the XPS spectra in between 101.6 and 102.8 eV. On vacuum annealing, the Si_{2p} peak position shifted towards higher energy and the Zn_{2p} peak shifted towards lower energy with the increase of annealing temperature.

In Fig. 2, a typical TEM photograph of as-grown Si/ZnO film prepared with 12 pieces of Si wafers (Si/Zn = 0.265) is presented. A distribution of nano-particles of size ranging 2–4 nm in the matrix can be observed. On vacuum annealing, the crystallinity of ZnO matrix increased, but no significant increase in the size of the nano-particles observed up to 600 °C. On annealing at temperatures 700 °C and above, the nano-particles aggregated to form micro-clusters. In Fig. 3, a typical TEM picture of the micro-clusters formed on annealing at 800 °C is shown. The twin lamellae pattern in most of the micro-clusters reveals their crystallinity and hence, the micro-clusters would be called as micro-crystals there after. A detailed study of the crystallinity and orientation of the micro-crystals have been reported else where [22]. For the samples annealed at 800 °C, the average size of the micro-crystals increased with the increase of Si content initially and then decreased for the films grown with more than eight pieces of Si wafers. For instance, the average size of the micro-crystals in

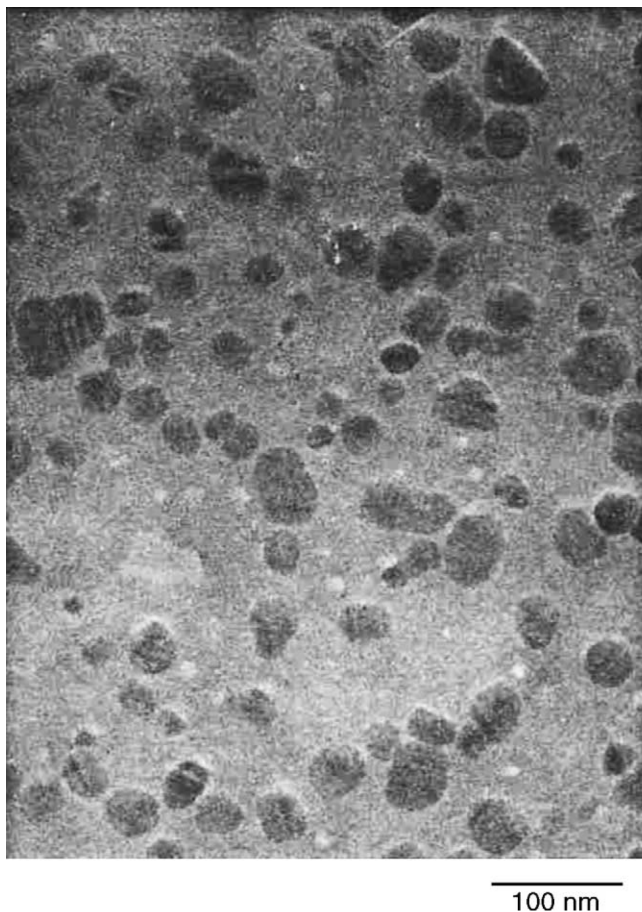

Fig. 3. TEM photograph of Si/ZnO film after annealing at 800 °C for 5 h.

the films prepared with four pieces of Si wafers was 38.2 nm, whereas, for films prepared with 12 pieces of Si wafers it was 32.4 nm. However, the number density of the micro-crystals increased with the increase of Si content in the films.

A complex evolution of different PL emissions is observed in the Si/ZnO composite films with different Si contents and with different temperatures of annealing. For as-grown samples, the integrated intensity of PL emission increased with the increase of Si content up to eight pieces of Si and thereafter decreased. However, on annealing, the PL emission increased with the increase of annealing temperature and with increasing Si content in the films. Analysing the PL spectra of all the samples (as-grown and annealed) we could identify five emissions. The emissions appeared at about 3.25, 2.8, 2.48, 2.24 and 1.97 eV. In Fig. 4, the PL spectra of Si/ZnO composite film grown with eight pieces of Si wafers and annealed at different temperatures are shown.

The PL emission peaked at around 3.25 eV, the most prominent one in as-grown films, is the band edge emission of ZnO [23] the intensity of which generally decreased with the increase of Si content in the films. The emission at about 2.8 eV appeared from the quartz glass substrate. The emission at about 2.48 eV which is most prominent in the films annealed at 400 °C was associated with recombination

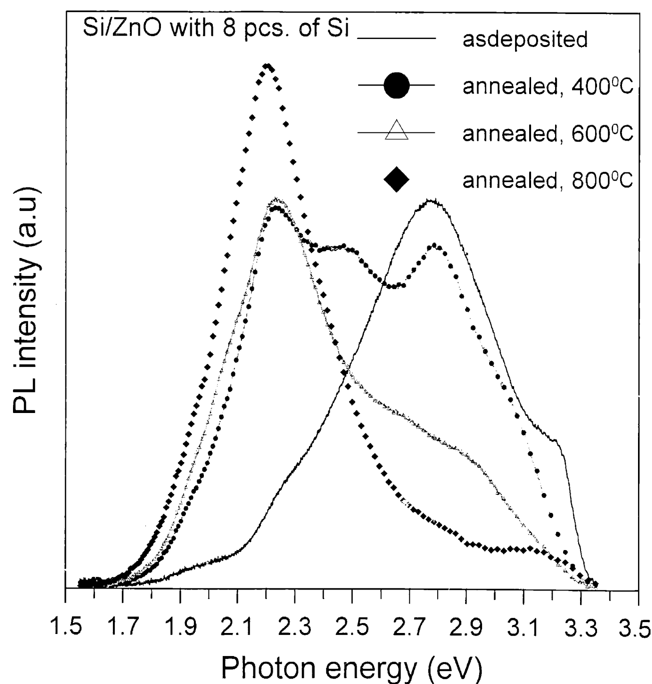

Fig. 4. PL spectra of Si/ZnO film grown with eight pieces of Si targets, annealed at different temperatures.

of singly ionized oxygen vacancy (V_O) electron with pump excited holes in the valence band [24] of ZnO. On thermal annealing, the shifts of Si_{2P} peak towards higher energy and Zn_{2P} peak towards lower energy in the XPS spectra were also indicative of oxidation of Si and hence creation of oxygen vacancy in ZnO [25,26]. However, on annealing at higher temperatures, the intensity of the PL emission reduced. The emission at about 2.24 eV, which is the prime interest of the present discussion, appeared broad in as-grown films. With the increase of annealing temperature and with increasing Si content in the films, the intensity increased significantly. It is noted that the full width at half maximum (FWHM) of the emission is decreased as the films were annealed at 700 °C or higher temperatures. For example, in Fig. 4, the PL (at about 2.24 eV) for the film annealed at 600 °C with a FWHM of about 0.5 eV and the same emission for the film annealed at 800 °C with a FWHM of about 0.4 eV. Though a direct correlation between the energies of the observed emission bands with the calculated photon energies of interband transitions in Si nano-crystals [27,28] is not possible in the present case, the observed PL energies and PL broadening with reduction of crystallite size can be explained by a model [29] involving absorption in the quantum confined Si cores, and emission due to transitions between dangling bonds or defect states in the oxidized outer layers of the nano-particles and micro-crystals.

Though, the XPS study could not reveal the Si_{2P} emission corresponding to elemental state of Si, as the technique gives information only from about 2–3 nm depth from the surface, there is a good possibility of retaining a non-oxidized Si core in the SiO_X capped nano-particles or micro-crystals

in the samples [30,31]. Our infrared absorption spectroscopy results on the composite films revealed the presence of elemental Si core in trimer cluster form [32]. With the increase of annealing temperature the ratio of SiO_X to Si increased and the Si_{2P} peak position shifted towards higher energy.

With the increase of annealing temperature up to 600 °C we could not detect any significant change in nano-particle size in the films. An increase of PL emission with the increase of annealing temperature is observed. No detectable shift of the peak position observed up to 600 °C annealing temperature. However, a small red shift of the peak is noticed for the annealing at 800 °C, at which temperature, nano-particles aggregated to form micro-crystals. With the increase of Si content in the films, the intensity of the emission increased. From the XPS and PL results we can assume that the formation of the Si oxide outer layer has been established even in unannealed samples. This SiO_X layer had a significant amount of Si and oxygen dangling bonds, thus a non stoichiometric Si/O ratio. Annealing at high temperatures passivated the dangling bonds, therefore achieving a more stoichiometric Si/O ratio (X increased towards 2), leading to improve PL intensity without any accompanying PL peak shift. The emission process is usually sensitive to different trapping states [33]. Several PL peaks recorded at around 1.7–1.9, 2.2–2.5 and 2.6–3.1 eV have been reported for different types of oxygen-related defects in Si oxide [34–36]. In our samples, the emissions from SiO_X are dominated by defect centers in the oxide. However, a simple band-to-band recombination mechanism within the Si cores cannot be ruled out. A small red shift of the 2.24 eV PL band and the subsequent reduction of FWHM for the films annealed at 800 °C (Fig. 4) justify our explanation. On annealing at 800 °C, a red shift of the PL peak is expected due to band-to-band recombination process. But due to the existence of surface related traps with energy levels extending into the energy gaps, there is a possibility of photo-generated carriers (in the conduction and valence bands of the dots) getting trapped by, and subsequently recombined through, these gap states [37–41]. A PL red shift with increasing dot size is possible, since the carriers generated in bigger dots may have access to gap states with trapping energies lower than the energy gap of the smaller dots. Decrease of PL band width with the increase of dot size is also expected as the carriers generated in bigger dots may also have access to gap states with much higher trapping energies. So, depending on the relative densities and recombination efficiencies of the different surface states involved, a reduction of PL broadening may accompany the PL red shift for the bigger dots. A similar observation has been made by Dinh et al. [29] for their oxygen passivated Si nano-crystals.

In Fig. 5, the evolution of 2.24 eV PL emission for the films containing different Si content and annealed at 800 °C is presented. The increase of emission intensity with an increase of Si content in the films is evident. There appeared a small peak shift between the emissions from the films prepared with eight and 16 pieces of Si targets, which might be due to the difference in the average size value of the micro-crystals in the films. However, it was difficult to correlate this small peak shift with the change of size of the microcrystallites. The increase of emission intensity with the increase of Si content in the films is expected as the number density of micro-crystals is high for the higher Si content films. In all the films, a PL emission at about 1.97 eV is observed. A band very close to this energy (at around 2.0 eV) was ascribed to the electron-hole recombination in Si-rich SiO_2 by Shimizu-Iwayama et al. [42]. Si excess defects formed near SiO_X are responsible for the emission. Very recently, Kabashin and Meunier [43] have also detected the PL bands around 2.0–2.3 eV and 1.95 eV for Si/SiOx prepared by UV and IR laser-induced treatments of Si, respectively.

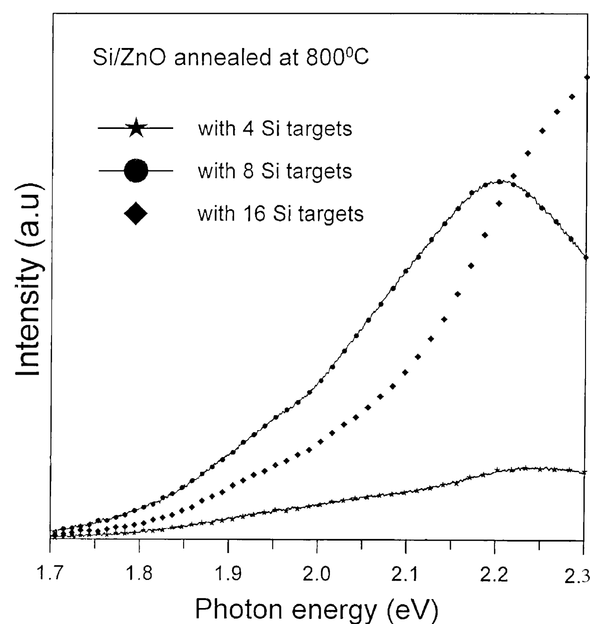

Fig. 5. Evolution of 2.24 eV PL emission for the films prepared with different Si targets and annealed at 800 °C.

The Raman spectra of most of the samples are dominated by PL emissions. In Fig. 6, Raman spectrum for a sample prepared with eight pieces of Si targets and annealed at 400 °C is shown. Most of the Raman emissions in the samples appeared with in 300 and 1300 cm^{-1} frequency range. None of the samples revealed the Si–Si Raman line, which generally peaked at about 520 cm^{-1}. In Fig. 7, the evolution of different Raman lines in the films with different silicon content and annealed at 800 °C is presented. A broad emission extending from 200 to 540 cm^{-1} is revealed for all the samples. The emission revealed a complex evolution on annealing which might be the result of annealing on the combined emissions from quartz glass and ZnO film.

The emission appeared at about 580 cm^{-1} is attributed to the E_1(LO) mode of ZnO. Generally the E_1(LO) mode does show resonance Raman enhancement in stoichiometric ZnO [44]. With the increase of Si content in the films and/or with the increase of annealing temperature, this peak became less intense, broader and ultimately vanishes. Such evolution

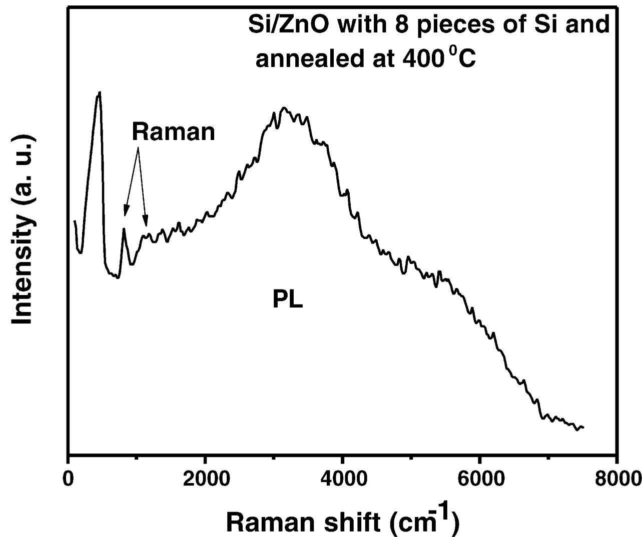

Fig. 6. Room temperature Raman spectrum for a film prepared with eight pieces of Si targets and annealed at 400 °C.

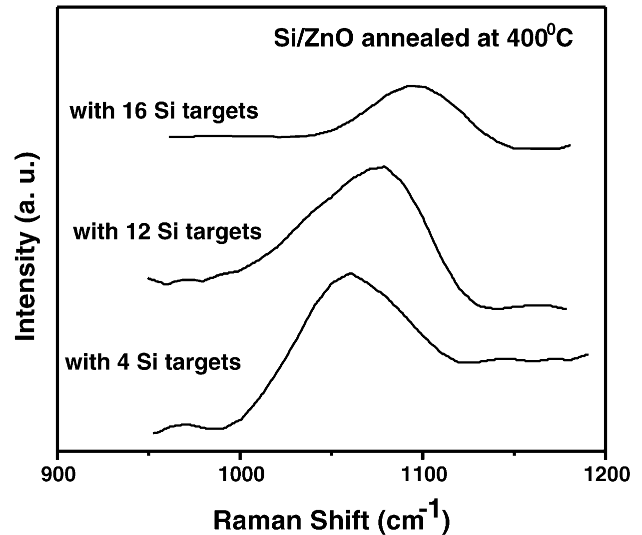

Fig. 8. Evolution of $TOAS_1$ Raman emission with the increase of Si content. All the films were annealed at 400 °C for 5 h.

of this peak might be due to impurity states introduced by excess zinc in the films. A zinc rich film in the present case is formed due to oxidation of dispersed silicon. With the increase of annealing temperature, the increase of excess zinc and hence increase of V_O centers in the films also supported by the lower energy shift of Zn_{sp} emission in the XPS spectra. A similar reduction of emission intensity of this peak with thermal annealing has also been observed by Exarhos and Sharma [23] for their zinc excess ZnO films. To confirm the origin of this emission a Raman spectrum of an unannealed ZnO film (about 1 μm thick, deposited on quartz glass) is measured and presented in Fig. 7 (the bottom curve). The emission at around 810 cm^{-1} can be associated with the Si-O-Si symmetric stretching (SS) vibrational mode [16]. The broadness of this emission may be arising due to its LO–TO splitting [45] which is not resolved in the present experiment. With the increase of Si content in the films, the emission became broader.

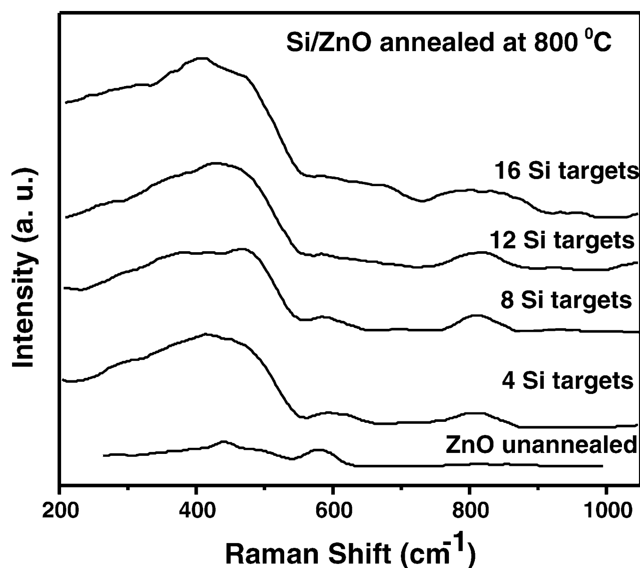

Fig. 7. Evolution of different Raman peaks in the films with different Si content annealed at 800 °C. The Raman spectrum for an unannealed ZnO film (t 1 μm) is presented at the bottom.

A broad emission band appeared at about 1065 cm^{-1} for the films prepared with four pieces of Si targets, which gradually shifted to 1085 cm^{-1} with the increase of Si content. In Fig. 8, the evolution of this band with the increase of Si content in the films is presented. The emission is generally assigned to the TO mode of the in phase asymmetrical stretching (AS_1) motion of the O atom along a line parallel to the axis through the two Si atoms [45,46]. The shift of the vibrational frequency with the change of silicon content in the films manifests a change in oxide composition [47–49] and an induction effect in which the chemical environment at each of the silicon atoms of the Si-O-Si linkage can promote the Si-O-Si vibration frequency [50]. As the oxide moves off stoichiometry ($X < 2$), the Si atoms have a higher probability of having one or more silicon neighbors and this shifts the Si-O-Si stretching frequency. The broadening of the band is a manifestation of a statistical distribution of different bonding arrangement at each Si atom site. As the Si atoms in our films were in the suboxide composition, the sharpness of the emission was low and the distinction between $TOAS_1$ and $TOAS_2$ transitions was impossible. However, a shift towards higher frequency with the increase of Si content in the films indicative of a higher order oxidation state of Si in the films with higher Si content [47–49].

4. Conclusions

Si/ZnO nanocomposites are prepared successfully by r.f. co-sputtering technique. With the increase of Si content in the

as-grown films, the number density of the nano-particles increased retaining their size more or less same. On thermal annealing up to 600 °C in vacuum, the size of the nano-particles did not change considerably. However, on thermal annealing, due to passivation of oxygen dangling bonds in SiO_X the PL intensity increased. The nano-particles aggregated to form micro-crystals at and above 700 °C. The Si in the films remained in the suboxide [SiO_X ($0 < X < 2$)] state. With the increase of annealing temperature, the oxidation state of Si increased. The PL properties of oxidized Si nano-particles is controlled by the oxide defect states [27]. We believe, that the defect centers, rather than band-to-band recombination in the Si nanocrystalline cores, are more likely responsible for the PL emission at about 2.24 eV in our samples. However, a simple band-to-band recombination mechanism within the Si cores cannot be ruled out.

Acknowledgements

U P thanks JISTEC, Japan for the STA award. The work is partially supported by VIEP-SEP-CONACyT, México (Project No. II013I02).

References

[1] L.T. Canham, Appl. Phys. Lett. 57 (1990) 1046.
[2] K.H. Jung, S. Shin, T.Y. Hsieh, D.L. Kwong, T.L. Lin, Appl. Phys. Lett. 59 (1991) 3264.
[3] R.W. Fathauer, T. George, A. Ksendzov, R.P. Vasquez, Appl. Phys. Lett. 60 (1992) 995.
[4] Y. Ochiai, N. Ookubo, H. Watanabe, S. Matsui, Y. Mochizuki, H. Ono, S. Kimura, T. Ichihashi, Jpn. J. Appl. Phys. 31 (1992) 560.
[5] A. Nishida, K. Nakagawa, H. Kakibayashi, T. Shimada, Jpn. J. Appl. Phys. 31 (1992) 1219.
[6] J.M. Pérez, J. Villalobos, P. McNeil, J. Prasad, R. Cheek, J. Kelber, J.P. Estrera, P.D. Stevens, R. Glosser, Appl. Phys. Lett. 61 (1992) 563.
[7] S. Hayashi, K. Yamamoto, J. Lumin. 70 (1996) 352.
[8] R. Tsu, H. Shen, M. Dutta, Appl. Phys. Lett. 60 (1992) 112.
[9] C.H. Ferry, F. Lu, F. Namavar, N.M. Kalkhoran, R.A. Soref, Appl. Phys. Lett. 60 (1992) 3117.
[10] H. Morisaki, F.W. Ping, H. Ono, K. Yazawa, J. Appl. Phys. 70 (1991) 1869.
[11] Y. Maeda, N. Tsukamoto, Y. Yazawa, Y. Kanemitsu, Y. Masumoto, Appl. Phys. Lett. 59 (1991) 3168.
[12] S. Schuppler, S.L. Friedman, M.A. Marcus, D.L. Adler, Y.-H. Xie, F.M. Ross, Y.J. Chabal, T.D. Harris, L.E. Brus, W.L. Brown, E.E. Chaban, P.F. Szajowski, S.B. Christman, P.H. Citrin, Phys. Rev. B 52 (1995) 4910.
[13] Y. Kanzawa, T. Kageyama, S. Takeoka, M. Fujii, S. Hayashi, K. Yamamoto, Solid State Commun. 102 (1997) 533.
[14] Y. Uto, H. Kanemitsu, Y. Masumoto, T. Matsumoto, H. Mimura, Phys. Rev. B 48 (1993) 2827.
[15] Y. Kanemitsu, T. Ogawa, K. Shiraishi, K. Takeda, Phys. Rev. B 48 (1993) 4883.
[16] T. Shimizu-Iwayama, K. Fujita, S. Nakao, K. Saitoh, T. Fujita, N. Itoh, J. Appl. Phys. 75 (1994) 7779.
[17] B. Delley, E. Steigmeier, Phys. Rev. B 47 (1993) 1397.
[18] F. Huaxiang, Y. Ling, X. Xide, Phys. Rev. B 48 (1993) 10978.
[19] T. Sasaki, R. Rozbicki, Y. Matsumoto, N. Koshizaki, S. Terauchi, H. Umehara, Mater. Res. Soc. Symp. Proc. 457 (1997) 425.
[20] N. Koshizaki, K. Yasumoto, S. Terauchi, H. Umehara, T. Sasaki, T. Oyama, Nanostruct. Mater. 9 (1997) 587.
[21] G. Zhao, H. Kozuka, T. Yoko, Thin Solid Films 227 (1996) 147.
[22] U. Pal, N. Koshoizaki, S. Terauchi, T. Sasaki, Microscopy Microanal. Microstruct. 8 (1997) 403.
[23] G.J. Exarhos, S.K. Sharma, Thin Solid Films 270 (1995) 27.
[24] K. Vanheusden, C.H. Seager, W.L. Warren, D.R. Tallant, J.A. Voigt, Appl. Phys. Lett. 63 (1996) 403.
[25] J. Garcia Serrano, U. Pal, N. Koshizaki, T. Sasaki, Rev. Mex. Fis. 47 (2001) 26.
[26] J. García Serrano, N. Koshizaki, T. Sasaki, G. Martínez Montes, U. Pal, J. Mater. Res. 16 (2001) 3554.
[27] N.A. Hill, K.B. Whaley, Phys. Rev. Lett. 75 (1995) 1130.
[28] L.W. Wang, A. Zunger, J. Phys. Chem. 98 (1994) 2158.
[29] L.N. Dinh, L.L. Chase, M. Balooch, W.J. Seikhaus, F. Wooten, Phys. Rev. B 54 (1996) 5029.
[30] C.D. Wagner, W.M. Riggs, L.E. Davis, J.F. Moulder, G.E. Muilenberg, Hand-book of X-ray Photoelectron Spectroscopy, Perkin-Elmer Corp., Edn. Prairie, MN, 1979.
[31] L.N. Dinn, L.L. Chase, M. Balooch, L.J. Terminello, F. Wooten, Appl. Phys. Lett. 65 (1994) 3111.
[32] U. Pal, J. García Serrano, Solid State Commun. 111 (1999) 427.
[33] A. Kux, D. Kovalev, F. Koch, Thin Solid Films. 255 (1995) 143.
[34] S.M. Prokes, W.E. Carlos, Appl. Phys. Lett. 78 (1995) 2671.
[35] J.H. Stathis, M.A. Kastner, Phys. Rev. B 35 (1987) 2972.
[36] I.A. Movtchan, R.W. Dreyfus, W. Marine, M. Sentís, M. Autric, G. Lelay, N. Merk, Thin Solid Films 255 (1995) 286.
[37] F. Koch, V. Petrova-Koch, T. Muschik, J. Lumin. 57 (1993) 271.
[38] L. Tsybeskov, J.V. Vandyshev, P.M. Fauchet, Phys. Rev. B 49 (1994) 7821.
[39] S.M. Prokes, O.J. Glembocki, V.M. Bermudez, R. Kaplan, L.E. Friedersdorf, P.C. Searson, Phys. Rev. B 45 (1992) 13788.
[40] W.L. Wiison, P.F. Szajowski, L.E. Brus, Science 262 (1993) 1242.
[41] L. Tsybeskov, P.M. Fauchet, Appl. Phys. Lett. 64 (1994) 1983.
[42] T. Shimizu-Iwayama, S. Nakao, K. Saitoh, Appl. Phys. Lett. 65 (1994) 1814.
[43] A.V. Kabashin, M. Meunier, Mater. Sci. Eng. B 101 (2003) 60–64.
[44] J.M. Calleja, M. Cardona, Phys. Rev. B 16 (1977) 3753.
[45] C.T. Kirk, Phys. Rev. B 38 (1988) 1255.
[46] M.L. Naiman, C.T. Kirk, B.L. Emerson, J.B. Taitel, J. Appl. Phys. 58 (1985) 779.
[47] P.G. Pai, S.S. Chao, Y. Takagi, G. Lucovsky, J. Vac. Sci. Technol. A 4 (1986) 689.
[48] G. Lucovsky, P.D. Richard, D.V. Tsu, S.Y. Lin, R.J. Markunas, J. Vac. Sci. Technol. A 4 (1986) 681.
[49] M. Nakamura, Y. Mochizuki, K. Usami, Y. Itoh, T. Nozaki, Solid State Commun. 50 (1984) 1079.
[50] G. Lucovsky, Solid State Commun. 29 (1979) 571.